*Ivana Uzelac*
*Hrvoje Smoljanović*
*Bernardin Peroš*

ISSN 1333-1124
eISSN 1849-1391

# A NEW ALGORITHM FOR DYNAMIC ANALYSIS OF THIN PLATES IN THE COMBINED FINITE-DISCRETE ELEMENT METHOD

**Summary**

This paper presents a new numerical algorithm for a dynamic analysis of thin plate structures based on the combined finite-discrete element method (FDEM). A nonlinear analysis of thin plates subjected to static or dynamic load has been provided. The model uses 3-noded triangular finite elements and is implemented in the open source FDEM package - Yfdem. The performance of the new model on simple benchmark tests is presented.

*Key words:* *plates, 3-noded finite element, finite-discrete element method*

## 1. Introduction

In mechanical terms, thin plates resist transverse loads by means of bending, where flexural properties of a plate depend greatly upon its thickness in relation to other two dimensions. As is well known, the term 'thin plates' refers to the plate structures to which Kirchhoff-Love theory of plates can be applied. Given the wide engineering applications of thin plate structures, including civil, marine and aerospace engineering, and their positioning in the design, thin plates tend to be subjected to various dynamic and impact loads (flying debris, moving vehicles, wind gusts, seismic disturbances, vehicle impact etc.). Therefore, an extensive dynamic analysis of such structures is clearly called for. If a structural member is not initially flat, these structures are referred to as shells. If the thickness of a plate becomes so small that the structure is devoid of flexural rigidity, then they are referred to as membranes.

Since exact analytical solutions for plate bending problems are very limited [22], various numerical methods have been developed. The most commonly used numerical tool for the dynamic analysis of thin plate structures is the finite element method (FEM), which is based on triangular, rectangular or quadrilateral finite elements [3], [9], [23]. The Kirchhoff-Love theory called for a deployment of conforming triangular and rectangular elements. However, when the thickness of the plate is reduced in relation to its width, shear members become dominant in the stiffness matrix, causing an unrealistic increase in plate stiffness known as shear locking [5], [6], [8]. A solution emerged in the form of a selective and reduced integration approach as a response for overcoming the shear locking phenomenon [1], [4], [10]. Nowadays, due to a richer strain field and increased accuracy, in comparison to triangular and rectangular elements, quadrilateral finite elements are considered optimal.

However, they are more difficult to apply to a description of an arbitrary geometry and are more sensitive to mesh distortions than triangular finite elements.

Unlike the finite element method, the discrete element method (DEM) is the approach best suited for the analysis of discrete elements. The advantages of the FEM and the DEM are the basis of a combined finite-discrete element method FDEM [11].Within the framework of this method, interaction between any discrete elements is enabled, with each of them having their own finite element mesh. An explicit central difference integration scheme is used in order to resolve the equations of motion directly. This is combined with lumped nodal masses, meaning that there is no need for either stiffness or mass matrices to be assembled. A simulation of plate structures using the FDEM has been made using triangular prismatic [16] and spherical finite elements [19].

In this paper, a finite strain, large displacement numerical model for the dynamic analysis of thin plate structures has been proposed. The following chapter presents discretization of the problem and a detailed description of the membrane and transverse carrying mechanisms. Subsequently, numerical examples are presented and discussed, illustrating the performance of the proposed numerical model.

## 2. Proposed combined finite-discrete element formulation

### 2.1 Discretisation

A discretization with 3-noded finite elements has been adopted to create an efficient representation of an arbitrary geometry. Masses are lumped into the nodes of finite elements, as shown in Fig. 1.

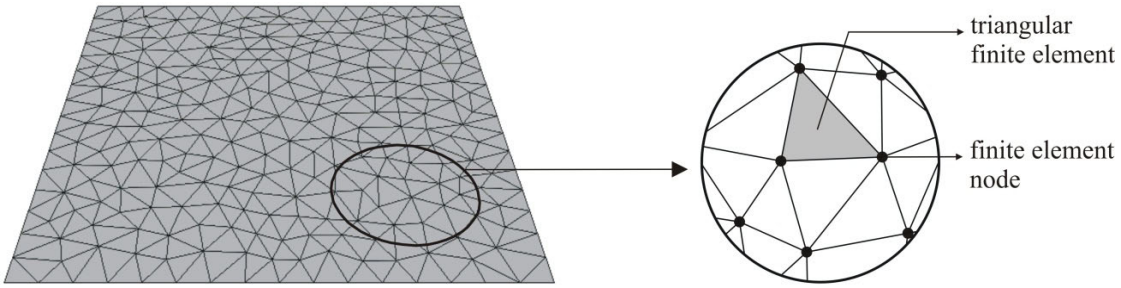


**Fig. 1** Discretization of plate structure

### 2.2 Membrane carrying mechanism

Change between the initial and the current nodal coordinates of each finite element defines membrane stresses. As shown in Fig 2, each node is described by its global initial Cartesian coordinates $(\bar{x},\bar{y},\bar{z})$ and global current Cartesian coordinates $(\tilde{x},\tilde{y},\tilde{z})$.

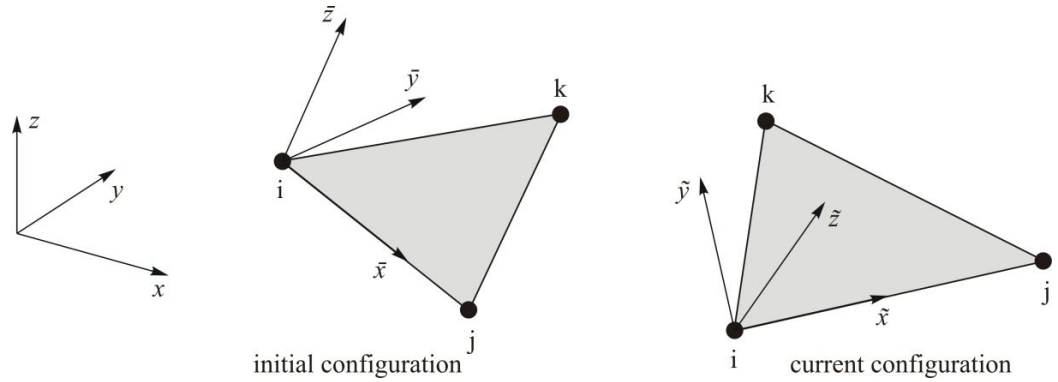


**Fig. 2** Initial and current coordinates of the nodes of a 3-noded finite element

Nodal coordinates of each finite element are transferred to a local 2D coordinate system, with a deformation gradient **F** [11]

$$\mathbf{F} = \begin{bmatrix} \tilde{x}_1 - \tilde{x}_0 & \tilde{x}_2 - \tilde{x}_0 \\ \tilde{y}_1 - \tilde{y}_0 & \tilde{y}_2 - \tilde{y}_0 \end{bmatrix} \begin{bmatrix} \bar{x}_1 - \bar{x}_0 & \bar{x}_2 - \bar{x}_0 \\ \bar{y}_1 - \bar{y}_0 & \bar{y}_2 - \bar{y}_0 \end{bmatrix}^{-1} \tag{1}$$

In order to improve the CPU efficiency while preserving consistent multiplicative decomposition, a rotated global coordinate system is adopted [7]. As the origin of the coordinate systems coincides with the first node of the element, this yields:

$$\mathbf{F} = \begin{bmatrix} \tilde{x}_1 & \tilde{x}_2 \\ \tilde{y}_1 & \tilde{y}_2 \end{bmatrix} \begin{bmatrix} \bar{x}_1 & \bar{x}_2 \\ \bar{y}_1 & \bar{y}_2 \end{bmatrix}^{-1} \tag{2}$$

Using the deformation gradient, the Green-St. Venant strain tensor is obtained as follows:

$$\mathbf{E} = \frac{1}{2}(\mathbf{F}\mathbf{F}^{\mathrm{T}} - \mathbf{I}) \tag{3}$$

Employing Hooke's law, the Cauchy stress tensor **T** is obtained according to

$$\mathbf{T} = \frac{E}{1+\nu}\breve{\mathbf{E}}_{\mathbf{d}} + \frac{E}{1-2\nu}\breve{\mathbf{E}}_{\mathbf{s}} + \bar{\mu}\mathbf{D} \tag{4}$$

where $E$ is the modulus of elasticity, $\nu$ is the Poisson ratio, $\breve{\mathbf{E}}_{\mathbf{d}}$ is the shape changing part and $\breve{\mathbf{E}}_{\mathbf{s}}$ is the volume changing part of the Green-St. Venant strain tensor, $\bar{\mu}$ is the damping coefficient and **D** is the rate of the deformation tensor [17]. Equivalent nodal forces are then integrated directly from traction forces along the edges of the finite element

$$\begin{bmatrix} f_{\tilde{x}} \\ f_{\tilde{y}} \end{bmatrix} = \mathbf{T} \begin{bmatrix} n_{\tilde{x}} \\ n_{\tilde{y}} \end{bmatrix} \tag{5}$$

where $n_{\tilde{x}}$ and $n_{\tilde{y}}$ present components of the geometric normal along the edge of the finite element. Each node takes half of the traction forces from neighbouring sides of the finite element.

## 2.3 Transverse carrying mechanism

Due to the deformation of the plate structure, change in the angle between adjacent finite elements occurs, as shown in Fig. 3.

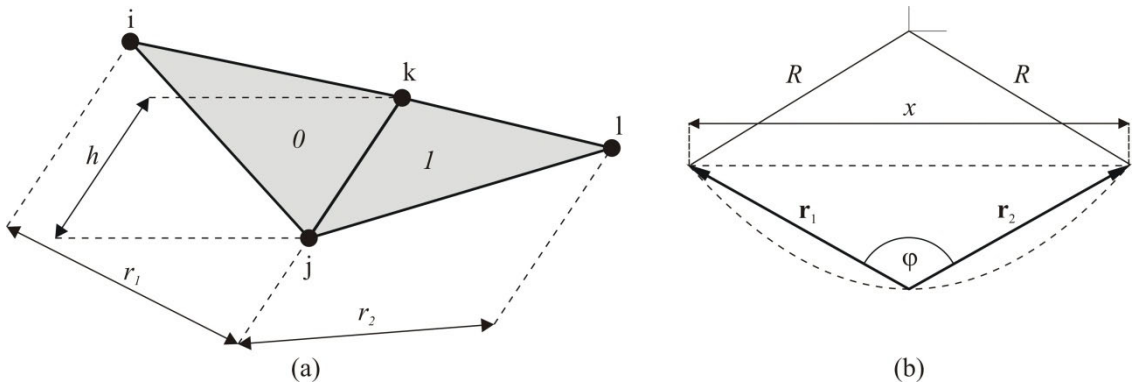


**Fig. 3** (a) Geometry of two neighbouring finite elements, (b) Angle between two neighbouring finite elements

Taking into account a mathematical expression for a curvature having 3 points, the initial curvature of the adjacent finite element is defined as:

$$\kappa_i = 2\frac{\sin\varphi_i}{x_i} \tag{6}$$

where $\varphi_i$ presents the initial angle between the finite elements and $x_i$ presents the initial distance $x$ shown in Fig. 3. Analogously, the current curvature is defined as:

$$\kappa_c = 2\frac{\sin\varphi_c}{x_c} \tag{7}$$

where $\varphi_c$ represents the current angle between the finite elements and $x_c$ represents the current distance $x$ shown in Fig. 3. Change in the curvature $\kappa$ between two adjacent finite elements is thus:

$$\kappa = \kappa_c - \kappa_i \tag{8}$$

The bending moment is calculated from the change in the curvature by using a constitutive law, as shown in Fig 4. For a linear, elastic material, the bending moment equals [22]

$$m = \mathrm{I}\left(\kappa + \nu\kappa_0\right) + \left(\dot{\kappa} + \nu\dot{\kappa}_0\right)\mu \tag{9}$$

where $\kappa_0$ represents the mean value of the change in the curvature in the direction orthogonal to $\mathbf{r}_1$ or $\mathbf{r}_2$, $\dot{\kappa}$ represents the velocity of the change in the curvature, $\dot{\kappa}_0$ represents the velocity of the change in the curvature in the direction orthogonal to $\mathbf{r}_1$ or $\mathbf{r}_2$, $\mu$ represents the damping coefficient, and $I$ is the bending stiffness given by the well-known expression:

$$I = \frac{Et^3}{12(1-\nu^2)} \tag{10}$$

where $t$ is the plate thickness.

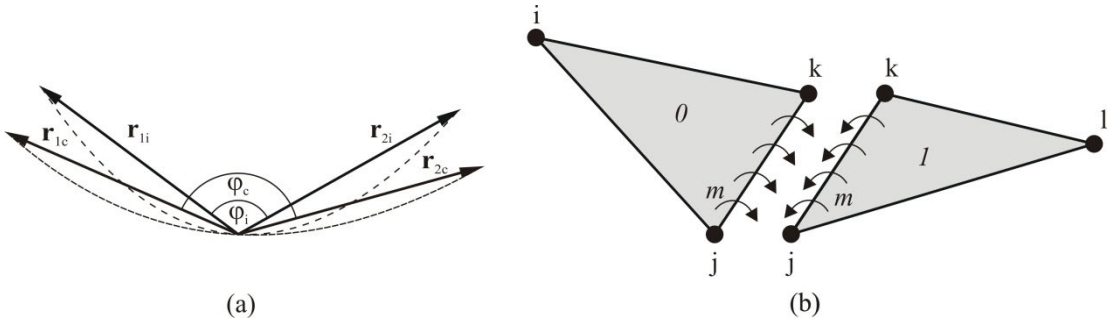


**Fig. 4** (a) Initial and current angle between finite elements, (b) Bending moment

The moment is converted into equivalent nodal forces **f**, which are perpendicular to the plane of the parent finite element, as shown in Fig. 5, with

$$f_i = \frac{m\,h}{r_{1c}}, \quad f_l = \frac{m\,h}{r_{2c}} \tag{11}$$

where $h$ is the length of the contact element, Fig. 3a. Forces acting on the nodes $j$ and $k$ are defined as:

$$f_{j0} = f_i \frac{d}{h}, \; f_{j1} = f_l \frac{b}{h} \tag{12}$$

$$f_{k0} = f_i \frac{c}{h}, \; f_{k1} = f_l \frac{a}{h} \tag{13}$$

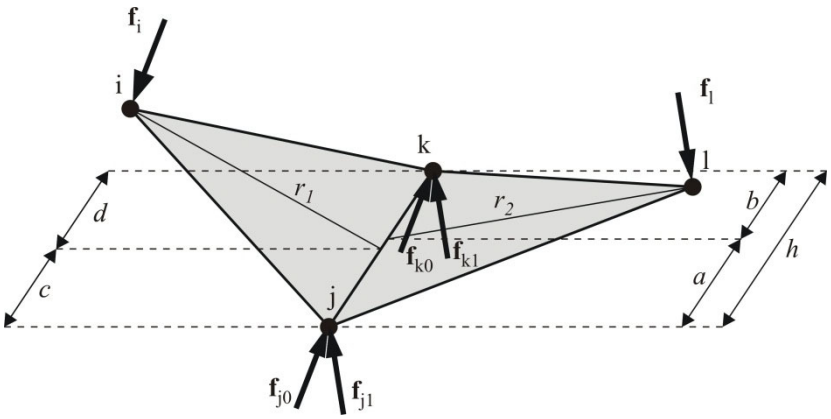


**Fig. 5** Bending moment presented with equivalent nodal forces

Forces due to the moment are then added to a global nodal force vector.

## 3. Numerical examples

### 3.1 Dumped vibrations of a simply supported round plate

In this example, a simply supported round plate was chosen in order to verify the static displacement of the plate under uniform load. The geometry of the plate and the finite element mesh are shown in Fig. 6. The finite element mesh consists of 1527 finite elements. Mechanical properties of the material used in this numerical analysis are E=70 GPa and material density ρ= 2500 kg/m3. Gravity constant g was assumed to be 10.0 m/s2. The thickness of the plate is 0.014 m.

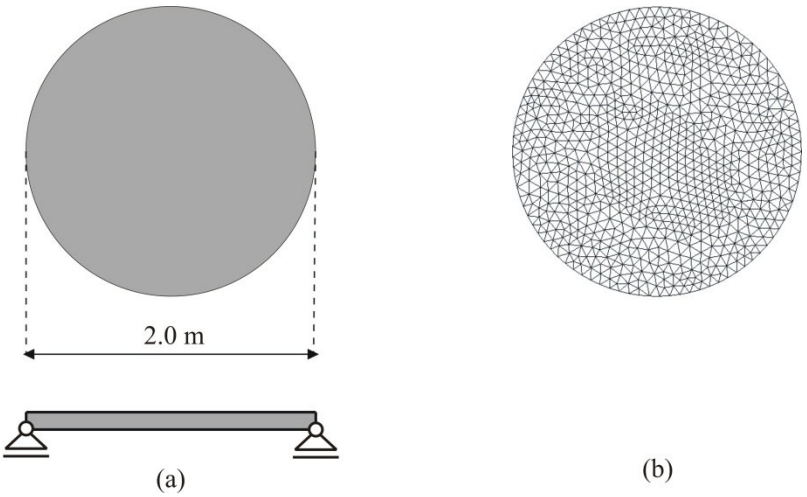


**Fig. 6** Geometry of the round plate

Starting from an initially flat geometry, the plate oscillates due to its self-weight, and, subsequently, as a result of dumping, finds an equilibrium position. Fig. 7 shows the mid-span

deflection of the plate obtained by adopting the dumping coefficient $\mu$ equal to 3.5 Nms. The numerical solution, which amounts to $d$=1.70 mm, shows excellent agreement of the result with the deflection obtained by the program Scia Engineer [20], where the deflection amounts to $d_s$=1.70 mm.

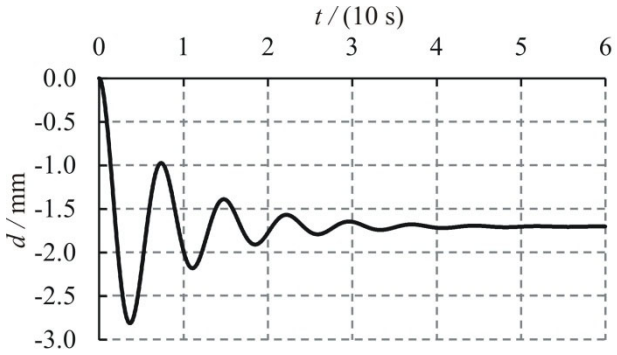


**Fig. 7** Time-displacement curve at the centre of the dumped round plate

## 3.2 Dynamic analysis of a simply supported square plate

In this example a square plate, simply-supported at all four edges, has been chosen in order to verify dynamic behaviour of the numerical model. Validation was performed by comparing the numerical with the analytical solutions, using three different mesh densities. The geometry of the plate and finite element meshes are shown in Fig. 8 and Fig. 9. Mesh densities are: M1 with 580 finite elements, M2 with 1160 finite elements and M3 with 2612 finite elements. The thickness of the plate was 0.014 m, and the mechanical properties are the same as in example 3.1.

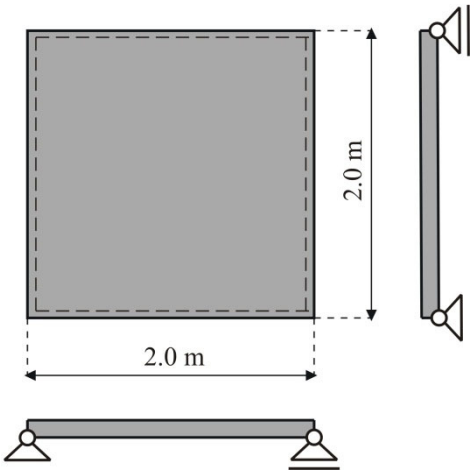


**Fig. 8** Geometry of the square plate

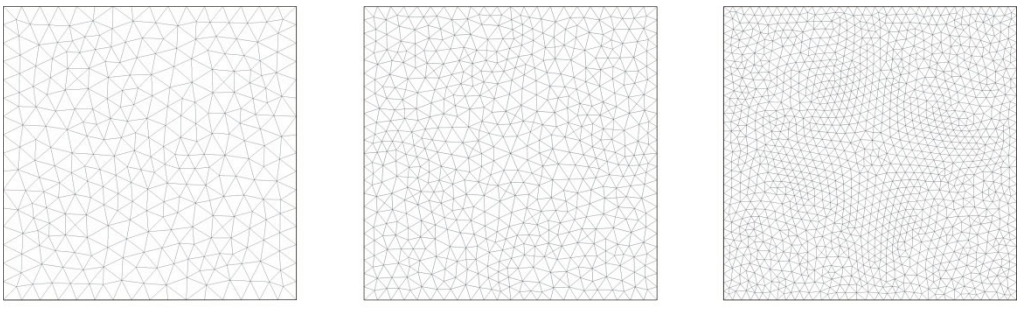


**Fig. 9** Discretisation of the square plate for different mesh roughness (a) M1 (b) M2 (c) M3

The vibrations are induced in a manner that the plate starting from initially flat geometry, due to its self-weight, oscillates around the equilibrium position. Fig. 10 shows the comparison of the analytical result for the displacement at the centre of the plate [22] with the response obtained by the FDEM model.

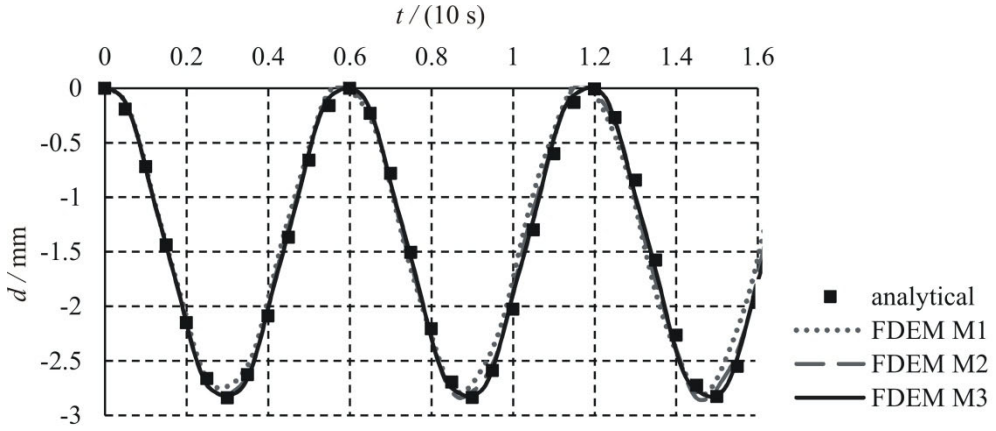


**Fig. 10** Time-displacement curve at the centre of the free oscillating square plate using meshes M1, M2 and M3

Table 1 shows the comparison of the dynamic displacement at the centre of the plate with the analytical solution by using M1, M2 and M3. It can be seen that the numerical model, with the increase in the number of finite elements, converges to the analytical solution.

**Table 1** Comparison between numerical and analytical solutions

| Discretization | Mid-span deflection (mm) | Error (%) |
|---|---|---|
| M1 | 2.75 mm | 0.033 |
| M2 | 2.80 mm | 0.014 |
| M3 | 2.82 mm | 0.007 |

## 4. Conclusion

This paper presents a new numerical algorithm for the static and the dynamic analysis of thin plate structures. It is based on the combined finite-discrete element method, with a novel approach to the transverse carrying mechanism and its implementation in Yfdem. For the sake of simplicity and efficiency, the structure has been discretised with 3-noded finite elements. Numerically, this reflects as a decrease in the size of a problem, which is computationally desirable.

The comparison between the analytical and the numerical results shows that the developed model successfully simulates bending stiffness as a result of inner moments. Also, by introducing a dumping coefficient, an equilibrium position can be easily obtained. Large displacements and large rotations are by default taken into account, as is the standard approach with the FDEM. Furthermore, the model is easily upgradable for performing impact simulations, which is yet another advantage of using the FDEM model.

It is worth pointing out that, in order for this model to be generalised for performing arbitrary shell structure analyses, a more detailed study is needed.

## REFERENCES

[1] Argyris, J., Papadrakakis, M., Mouroutis, Z. S., *Nonlinear dynamic analysis of shells with the triangular element TRIC*, Computer methods in applied mechanics and engineering, 2003, 192, 26-27, 3005-3038.

[2] Bangash, T., Munjiza, A., *Experimental validation of a computationally efficient beam element for combined finite-discrete element modelling of structures in distress*, 2003, Computational Mechanics, 30 (5-6), pp. 366-373.

[3] Bathe, K. J. *Finite element procedures*, Prentice-Hall, 1996.

[4] Bletziger, K.U., Bischoff, M., Ramm, E., *A unified approach for shear-locking-free triangular and rectangular shell finite elements*, Computers & Structures, 2000; 75(3): 321-334.

[5] Chapelle, D., Bathe K.-J., *The Finite Element Analysis of Shells – Fundamentals*, Springer, 2011.

[6] Dhondt, G., *The Finite Element Method fir Three-dimensional Thermomechanical Applications*, John Wiley & Sons, 2004.

[7] Divić, V., Uzelac, I., Peroš, B., *Multiplicative Decomposition Based FDEM Model for Membrane Structures*, Transactions of FAMENA, 2014, Vol.38, No.1.

[8] Dow, J. O., *A Unified Approach to the Finite Element Method and Error Analysis Procedures*, Academic Press, 1998.

[9] Hughes, T. J. R., *The finite element method, linear static and dynamic finite element analysis*, Prentice-Hall, 1987.

[10] Lee, P.S., Bathe, K.J., *Development of MITC isotropic triangular shell finite elements*, Computers & Structures, 2004;82:945–62.

[11] Munjiza, A., *The Combined Finite-Discrete Element Method,* John Wiley & Sons Ltd, 2004.

[12] Munjiza, A., Andrews. K.R.F., *NBS contact detection algorithm for bodies of similar size*, International Journal for Numerical Methods in Engineering, 1998, 43, 1,131–149.

[13] Munjiza, A., Knight, E., Rougier, E., *Computational Mechanics of Discontinua.* Wiley, 2011.

[14] Munjiza, A., Knight E., Rougier, E., *Large Strain Finite Element Method: A Practical Course*, Wiley, 2014.

[15] Munjiza, A., Latham, J.P., *Some computational and algorithmic developments in computational mechanics of discontinua*, Philosophical Transactions of the Royal Society A: Mathematical, Physical and Engineering Sciences, 362 (1822), pp. 1817-1833, 2004.

[16] Munjiza, A., Lei, Z., Divić, V., Bernardin, P., *Fracture and fragmentation of thin shells using the combined finite discrete element method*, Internationa Journal for Numerical Methods in Engineering, 2013, 95, 6, 478–498.

[17] Munjiza, A., Owen, D.R.J., Crook, A.J.L., *An M(M−1K)m proportional damping in explicit integration of dynamic structural systems*, International Journal for Numerical Methods in Engineering, 1998, 41, 7, 1277–1296.

[18] Munjiza, A., Rougier, E., John, N.W.M., *MR linear contact detection algorithm*, International Journal for Numerical Methods in Engineering, 2006, 66, 1, 46–71.

[19] Rousseau, J., Frangin E., Marin, P., Daudeville, L., *Multidomain finite and discrete elements method for impact analysis of a concrete structure*, Engineering Structures, 2009, 31, 11, 2735–2743.

[20] Scia Engineer 14, Nemetschek Group, Munich, 2014.

[21] Smoljanović, H., Živaljić, N., Nikolić, Ž., *A combined finite-discrete element analysis of dry stone masonry structures*, Engineering Structures, 2013, 52, 89–100.

[22] Ventsel, E., Krauthammer, T., *Thin Plates and Shells Theory, Analysis and Applications*, Marcel Dekker, Inc., 2001.

[23] Zienkiewicz, O.C., Taylor, R.L., *The Finite Element Method, Fifth edition*, McGraw-Hill, 2000.

Submitted: 11.11.2014

Accepted: 27.5.2015

Ivana Uzelac
Hrvoje Smoljanović
Bernardin Peroš
Fakultet građevinarstva, arhitekture i geodezije
Matice hrvatske 15
21000 Split